Multi-strain disease dynamics on metapopulation networks

Matthew Michalska-Smith[1,2], Kimberly VanderWaal[1], Montserrat Torremorell[1], Cesar Corzo[1], and Meggan E Craft[1]

[1]Department of Veterinary Population Medicine, University of Minnesota, St. Paul, MN USA
[2]Department of Plant Pathology, University of Minnesota, St. Paul MN, USA

October 28, 2022

1   Abstract

A much-updated version of this work is now available published open-access at *Scientific Reports*: https://www.nature.com/articles/s41598-022-12774-5

Many pathogens have clusters of variation in their genotypes that we refer to as strain structure. Importantly, when considering related pathogen strains, host immunity to one strain is often neither independent from nor equivalent to immunity to other strains. This partial cross-reactive immunity can thus allow repeated infection with (different strains of) the same pathogen and shapes disease dynamics across a population, in turn influencing the effectiveness of intervention strategies. To better understand the dynamics governing multi-strain pathogens in complex landscapes, we combine two frameworks well-studied in their own right: multi-strain disease dynamics and metapopulation network structure. We simulate the dynamics of a multi-strain disease on a network of populations connected by migration and characterize the joint effects of disease model parametrization and network structure on these dynamics. We find that the movement of (partially) immune individuals tends to have a larger impact than the movement of infectious individuals, dampening infection dynamics in populations further along a chain. When disease parameters differ between populations, we find that dynamics can propagate from one population to another, alternatively stabilizing or destabilizing destinations populations based on the dynamics of origin populations. In addition to providing novel insights into the role of host movement on disease dynamics, this work provides a framework for future predictive modelling of multi-strain diseases across generalized population structures.

1   Introduction

Many of the most impactful infectious diseases that affect humans (influenza, malaria, human papillomavirus, *etc.*), livestock (porcine reproductive and respiratory syndrome, foot-and-mouth disease, *etc.*), and wildlife (anthrax, plague, *etc.*) have clusters in their population-genetic variability that we classify as strains. This variation in pathogen genotype is often associated with differences in phenotype, which can have profound effects on the efficacy of host immune defenses. While the human immune system is usually capable of preventing re-infection—*i.e.* infection with something to which it has been previously exposed—sufficient, divergent evolution among pathogen strains can

26 reduce the ability of the host to recognize, and thus mount an immunological response to, subsequent
27 exposures. In some cases, this change is not sufficient to completely avoid recognition by the host's
28 immune system, yielding an immune response that is neither as strong as it would be in the case
29 of re-exposure to the same strain, nor as weak as in the case of exposure to a novel pathogen.
30 This partial cross-reactive immunity can likewise lead to reduced transmissibility, affecting disease
31 dynamics across the population.

32 While the study of multi-strain diseases goes back decades (1; 2), the resulting modelling frame-
33 work has not yet been generalized to a collection of sub-populations connected through host move-
34 ment, *i.e.* a metapopulation (but see (3)). Initially introduced through the concepts of island
35 biogeography (4), the network approach of metapopulations can be applied to a variety of systems,
36 including human movement between cities, livestock transport between farms, and wildlife living
37 in fragmented natural habitats. In each case, there exist relatively high-density areas which are
38 connected to one another through a network of individuals' movement. A metapopulation frame-
39 work allows the application of network analyses to characterize patterns of connection within the
40 larger system, and can provide unique insights across scales.

41 Historically, metapopulation studies have been been divided into two main camps: those that mo-
42 del within-population dynamics and "cell occupancy" models. The latter of which, where only the
43 presence or absence of a given species within a population is recorded in a given timepoint (5), has
44 received much more theoretical attention. Importantly, cell occupancy models rest on an assump-
45 tion of temporal separation in which local dynamics occur on a timescale that can be treated as
46 instantaneous relative to that of the between-population dynamics (6). When considering patho-
47 gens in systems with relatively high migration rates, however, this assumption rarely holds, and the
48 presence-absence approach can significantly limit model accuracy (7; 8; 9).

49 The presence of metapopulation structure has been repeatedly associated with increased stabili-
50 ty (10; 11; 12). This is due in part to the ability of migration between asynchronous populations to
51 rescue temporarily low density populations from extinction (13). This is particularly relevant when
52 populations are undergoing cyclical or chaotic dynamics, where repeated instances of low density

3

53 are generally considered to be at greater risk of extinction than a population maintaining steady

54 state dynamics (14; 15).

55 Here, we build on the strain theory of host-pathogen systems proposed by (16), considering a scenario

56 where a collection of populations undergoing local dynamics are furthermore interconnected through

57 the movement of individuals between populations. We simulate disease dynamics on this system,

58 characterizing the effects of parametrization and network structure on these dynamics. This work is

59 divided into three sections: first, we explore a case of interconnected populations which have been

60 parametrized to display identical dynamics in the absence of host migration. Second, we consider

61 cases where parameters differ between populations. Finally, we explore the role of network structure

62 on disease dynamics in larger networks of connected populations.

63 2 Methods

64 2.1 Model framework for one population

65 We work from a system of ordinary differential equations which delineate a population into classes

66 based on current and past exposure to different strains of a pathogen. Pathogens with strain struc-

67 ture can differ in both the number of strains and the level of cross-reactive immunity afforded by

68 past exposure to similar strains. To model the number of strains, we signify a strain $i = \{x_1, x_2, \ldots,$

69 $x_n\}$ as a set of n loci, each of which can take on a finite number of alleles. For instance, a pathogen

70 with two loci (a and b) and two alleles at each loci has a total of four potential strains: $\{a_1, b_1\}$,

71 $\{a_1, b_2\}, \{a_2, b_1\}, \{a_2, b_2\}$. For cross-reactive immunity, we use a parameter γ which indicates the

72 degree of reduced susceptibility a host has to strains that are similar to (*i.e.* strains that share

73 at least one allele with one another) past exposures. Importantly, in this framework, the number

74 of strains is fixed and finite. While strains may go extinct over time, there is no process for the

75 generation of new strains or to re-introduce strains that had previously gone extinct (but see (16)).

76 The model consists of sets of three nested equations (one set for each strain i): y, z, and w. See (17)

77 for a more comprehensive discussion of the model framework, including a graphical representation.

4

y_i represents the proportion of the population currently infectious with strain i. z_i represents the proportion of the population that has been exposed to strain i. These individuals harbor complete immunity to future infections with strain i and include those currently infected, *i.e.* y_i, those that have recovered but were previously infectious, and those that were exposed, but protected from becoming infectious due to partial cross-protective immunity. Finally, w_i represents the proportion of the population which has been exposed to any strain j which has at least one allele in common with strain i (including strain i itself), *i.e.* $j \cap i \neq \emptyset$. These individuals have at least partial immunity to strain i. *N.b.* these equations are nested such that any individual in y_i is also in z_i and any individual in z_i is also in w_i, and $y_i \leq z_i \leq w_i \ \forall$ strain i. In traditional Susceptible-Infected (SI), Susceptible-Infected-Recovered (SIR), *etc.* single-strain mathematical frameworks: the y class is analogous to the I class, while w and z are composed of combinations of I and R classes. The susceptible population is not modelled explicitly in this framework.

Explicitly, these three equations (for a given strain i) are:

$$
\begin{aligned}
\frac{dy_i}{dt} &= \beta \left((1 - w_i) + (1 - \gamma)(w_i - z_i) \right) y_i - \sigma y_i - \mu y_i \\
\frac{dz_i}{dt} &= \beta(1 - z_i)y_i - \mu z_i \\
\frac{dw_i}{dt} &= \beta(1 - w_i) \sum_{j \ni j \cap i \neq \emptyset} y_j - \mu w_i
\end{aligned}
\tag{1}
$$

As above, we denote strains as subscripts and, in the equation for w_i, we sum over all strains j which share at least one allele with the focal strain i. β, σ, and μ are the infection, recovery, and death rates, respectively. γ (as mentioned above) is an indicator of the level of cross-reactive immunity gained by prior exposure to alleles in the target strain. Note that while we depict only one value per demographic parameter (*i.e.* all strains are functionally equivalent) for clarity of notation, these values could also be written to vary by strain (*e.g.* β_i).

Immunity in this framework is non-waning: exposure to a strain yields consistent protection from future infection over the lifespan of the individual. Moreover, this protection is trichotomous: an individual can either have no protection from a given strain (it has not seen any of the alleles

before), complete protection (it has seen this exact combination of alleles before), or a set point in-between according to the parameter γ (it has seen at least one, but not all alleles before). Put another way, we do not distinguish between loci, assuming that sharing an allele at one locus is functionally identical to sharing an allele at any other locus, or indeed all other loci except one.

2.2   Extensions to more than one population

Following (18), we model movement between populations using a dispersal matrix $\boldsymbol{\Delta} = \mathbf{A}$ - $\mathbf{E}$, where $\mathbf{A}$ is the weighted adjacency matrix containing elements A_{kl} indicating the proportion of population k (row) moving to population l (column) per unit time and $\mathbf{E}$ is a diagonal matrix representing emigration, where each entry $E_{kk} = \sum_{k=1}^{n} A_{kl}$ where n is the number of populations. Thus, the whole system can be depicted by a set of three equations per strain i per population k:

$$
\begin{aligned}
\frac{\mathrm{d}y_{i,l}}{\mathrm{d}t} &= \beta\left((1 - w_{i,k}) + (1 - \gamma)(w_{i,k} - z_{i,k})\right)y_{i,k} - \sigma y_{i,k} - \mu y_{i,k} + \sum_{k} \Delta_{kl}y_{i,k} \\
\frac{\mathrm{d}z_{i,l}}{\mathrm{d}t} &= \beta(1 - z_{i,k})y_{i,k} - \mu z_{i,k} + \sum_{k} \Delta_{kl}z_{i,k} \\
\frac{\mathrm{d}w_{i,l}}{\mathrm{d}t} &= \beta(1 - w_{i,k}) \sum_{j \ni j \cap i \neq \varnothing} y_{j,k} - \mu w_{i,k} + \sum_{k} \Delta_{kl}w_{i,k}
\end{aligned}
\tag{2}
$$

Where $\boldsymbol{\Delta}^{\mathrm{T}}$ signifies the transpose of $\boldsymbol{\Delta}$, and each equation from Section 2.1 is now additionally indexed according to population and has an additional term to account for migration between populations. While in principle the elements of $\boldsymbol{\Delta}$ can take any value [0, 1], signifying a (continuous) movement of between 0 and 100% of individuals, for simplicity we use a constant value δ for the strength of each movement, *i.e.* for each non-zero off-diagonal element of $\boldsymbol{\Delta}$. Sensitivity to this value is explored in the supporting information (Fig S2).

This framework can be applied to a metapopulation of arbitrary size and complexity, with the number of equations being linearly related to the number of populations. The dynamics of each population are governed by a set of three equations per pathogen strain, and these equations are interlinked within populations by partial, cross-reactive immunity, and between populations through a movement network. The total number of differential equations for any given system will

6

121   be three times the number of strains multiplied by the number of populations in the metapopulation.

2.3   Simulation Procedure

All simulations were carried out in Julia version 1.3.0 (19), with graphics produced using the ggplot2

package (20) in R version 3.6.1 (21). For simplicity of presentation, we fix the values of all variables

other than β (the infection rate) and $\boldsymbol{\Delta}$ (the network of movement information) to be identical for

all populations in the metapopulation. To demonstrate the variety of dynamics obtainable in this

modeling framework, we vary

$$\tilde{R}_0 = \frac{\beta}{\sigma + \mu + E_{kk}},$$

123   where $E_{kk} = -\Delta_{kk}$, as noted above, signifies the total outgoing movement from the population of

124   interest. We add a ˜ over R_0 to denote that this is an approximation of the true reproductive

125   number, the precise form of which would additionally take into account the inflow of infectious

126   individuals from other populations. We additionally vary $\boldsymbol{\Delta}$ according to the number and inter-

127   connectedness of the populations. For the figures of the main text, we utilize a strain structure of

128   two loci, each with two alleles. Sensitivity to these parameter choices is explored in the supporting

129   information (Fig S3).

2.3.1   Populations with identical parametrizations

131   To assess the effect of migration on population dynamics, we first consider the simplest case of a

132   set of populations sharing the same disease parametrization: β such that $\tilde{R}_0 = 2$, $\sigma = 8$, $\mu = 0.1$,

133   and $\gamma = 0.66$. We use a movement network described by a chain of populations, *i.e.* A→B→C→D

134   or

$$\boldsymbol{\Delta} = \begin{bmatrix} -\delta & \delta & 0 & 0 \\ 0 & -\delta & \delta & 0 \\ 0 & 0 & -\delta & \delta \\ 0 & 0 & 0 & 0 \end{bmatrix},$$

7

135 where δ = 0.05, and ask how the dynamics of populations further down the chain (*i.e.* B, C, D)

136 differ from those of the origin population (*i.e.* A), recalling that, without migration, all populations

137 would have identical dynamics.

2.3.2 Populations with varying parametrizations

139 We next consider the case where parameters differ between connected populations, we restrict our

140 consideration to a system of two populations, identical in all respects other than the parameter β,

141 which is set to either induce a steady state of coexisting strains (β such that $\tilde{R}_0 = 5$ in population

142 A) or cyclically coexisting strains (β such that $\tilde{R}_0 = 2$ in population B). We then display three

143 potential patterns of connection: no migration (left column), A→B (middle column), and B→A

144 (right column). Specifically, we set

$$\mathbf{\Delta} = \begin{bmatrix} 0 & 0 \\ 0 & 0 \end{bmatrix}, \mathbf{\Delta} = \begin{bmatrix} -\delta & \delta \\ 0 & 0 \end{bmatrix}, \text{and }, \mathbf{\Delta} = \begin{bmatrix} 0 & 0 \\ \delta & -\delta \end{bmatrix},$$

145 respectively, again with δ = 0.05, σ = 8, μ = 0.1, and γ = 0.66.

146 To address the case of multiple origin populations feeding into a single destination population, we

147 consider a system of three populations: A→C←B, or

$$\mathbf{\Delta} = \begin{bmatrix} -\delta & 0 & \delta \\ 0 & -\delta & \delta \\ 0 & 0 & -\delta \end{bmatrix},$$

148 where populations A and C have β corresponding to an $\tilde{R}_0 = 5$, but population B has β correspond-

149 ing to an $\tilde{R}_0 = 2$; all other parameters as above.

2.3.3 Larger network structure

151 Finally, we characterize the role of global network structure through considering the impact of

152 degree distribution on a few summary statistics of system-wide disease burden: the mean proportion

8

153 of infectious individuals (area under the currently infectious (*i.e.* y) curve), the mean level of strain-
154 specific immunity (average z value), and the mean time between epidemic peaks (*i.e.* between local
155 maxima in y) over the course of the final 33% of the simulation. We omit the initial period of the
156 simulation to reduce the impact of transient dynamics.

157 We perform 100 simulations for each of five generic network ensembles each with 25 populations
158 and a connectedness of approximately 0.15. Specifically, we examine Erdős-Rényi (links randomly
159 assigned between populations), stochastic block (a metapopulation consisting of two groups of po-
160 pulations which have high migration within the group, but low migration to populations in the other
161 group), tree-like (where there are many chains of populations and no potential for cycles), Barabasi-
162 Albert (a scale-free network in which there tends to be a few populations with very many links,
163 and many populations with few links), and Watts-Strogatz (a small-world network structure which
164 is produced by partially re-wiring a spatially connected grid of populations) network structures. To
165 generate these networks, we utilize functions from the tidygraph R package (22), except in the case
166 of the tree and Watts-Strogatz configuration for which we use custom algorithms. Note that we use
167 a parameter of attachment of 4 for the Barabasi-Albert random graphs. This allows for comparable
168 connectences to the other random graphs as well as distinguishing these randomizations from trees
169 (as would result from a default parameter of attachment of 1). In all cases, each migration strength
170 is set to a constant $\delta = 0.01$, only the pattern of connections varies. Each population is assigned
171 a random β value corresponding to a $\tilde{R}_0$ between [1, 6]. These results are qualitatively similar if
172 instead every population is assigned the same value of β.

173 All code is made available on GitHub: https://git.io/JeqMc.

3   Results

175 In the following sections, we provide figures to demonstrate the effect of metapopulation structure on
176 disease dynamics. In these figures, we plot a time series for each of three subsets of the population:
177 those currently infected with a particular strain of the pathogen, those having (complete) specific
178 immunity against the focal strain, and those who have at least partial cross-reactive immunity to

the focal strain, due to past exposure to a similar strain (see Methods). Populations differ in their β (and thus R_0) value. This can be considered, for example, as differences in population density, which affects the probability of disease transmission. We only depict one representative strain in each plot for visual clarity and parametrize the model such that all strains are functionally equivalent (*i.e.* they all have the same transmission and recovery rates within any given population).

3.1 Cyclical dynamics are dampened along chains in the metapopulation network

We found that even when all populations share the same parametrizations and initial conditions, that populations further along network chains have reduced proportions of currently infectious individuals and dampened oscillatory dynamics compared to those they would exhibit in isolation (Fig 1). This is due to the movement of (partially) immune individuals between the populations, increasing the proportion of individuals with specific and cross-reactively immunity in populations further along the chain. While infectious individuals move at an equal rate, the proportion of the population that is currently infectious at any given time is much smaller than the proportion with immunity.

3.2 Dynamics propagate through metapopulation networks

We found that in the case of a simple chain of populations, the dynamics of destination populations can be overridden by the dynamics of origin populations (Fig 2). Interestingly, this is true both of cyclical dynamics overruling stable dynamics and *vice versa*, though the required amount of migration differs according to the origin and destination dynamics (see supporting information Fig S2). This migration can also allow for strain coexistence even in populations where the local parameters would suggest extinction of one or more strains.

The issue of dynamics propagation gets more complicated when there are multiple, varying origin populations for a given destination population. We found that there is a hierarchy of dynamics in their propagation through the network: when there are origin populations with both cyclical and steady state dynamics, the destination population inherits the cyclical dynamics (Fig 3), albeit
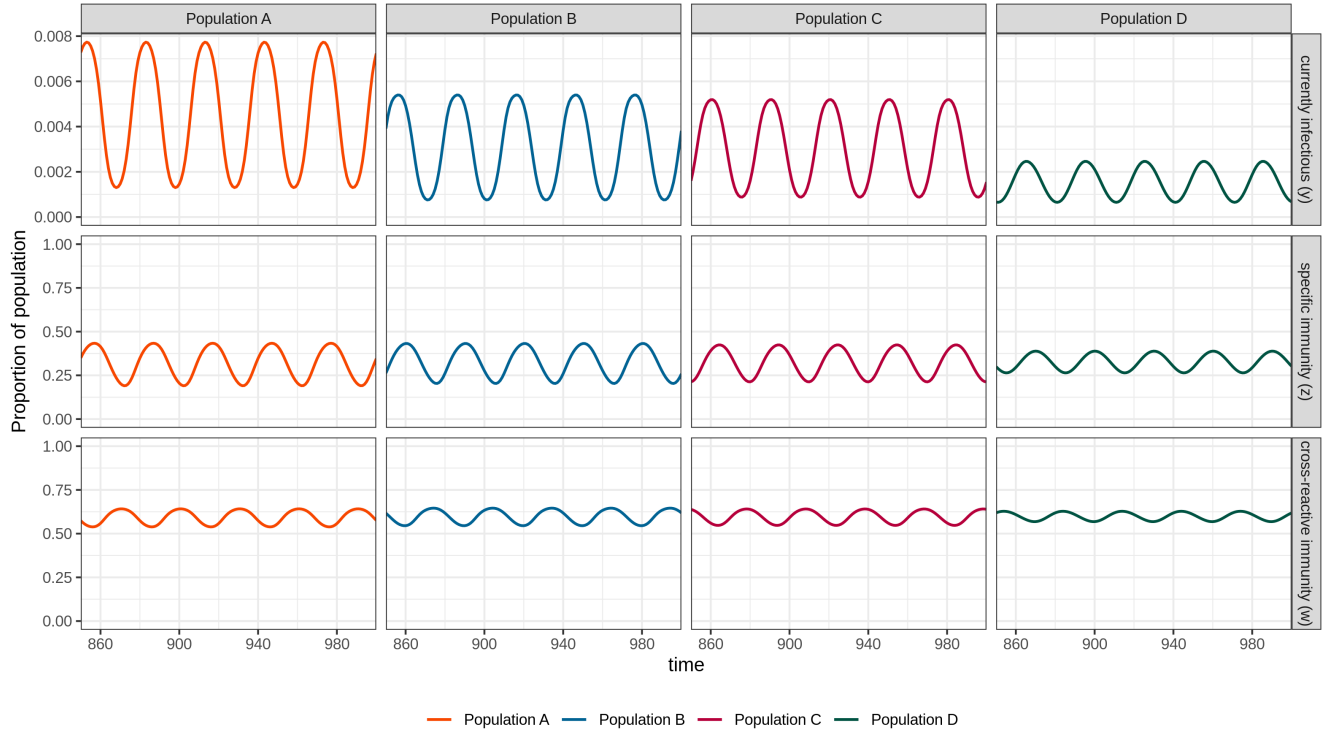
10

Figure 1: Connecting multiple populations with the same parameters results in reduced pathogen prevalence and dampened cycles in populations further down the chain. Here, populations are connected such that $A \rightarrow B \rightarrow C \rightarrow D$. Each column indicates a population, while each row is one of the three population classes laid out above and in the Methods, *i.e.* those currently infectious with the given strain, those with (complete) specific immunity to the given strain, and those with partial cross-protective immunity to the given strain. The mean level of immunity (both specific (middle row) and cross-reactive (bottom row)) increases in each sequential population, while the mean level of currently infectious individuals (top row) decreases. All populations have parameters $\sigma = 8$, $\mu = 0.1$, $\delta = 0.05$, $\gamma = 0.66$ and a β chosen to make $\tilde{R}_0 = 2$ for all populations. We use a two-loci, two-allele strain structure, but show only one strain for clarity (but see supporting information Fig S1).

205 dampened from what they would have been without migration from a steady state population.

206 This asymmetrical inheritance is robust to imbalance in the relative contributions of the origins. Put

207 another way, if just one of many origin populations (or a small proportion of the total movement)

208 has cyclical dynamics, the destination population will also have cyclical dynamics.
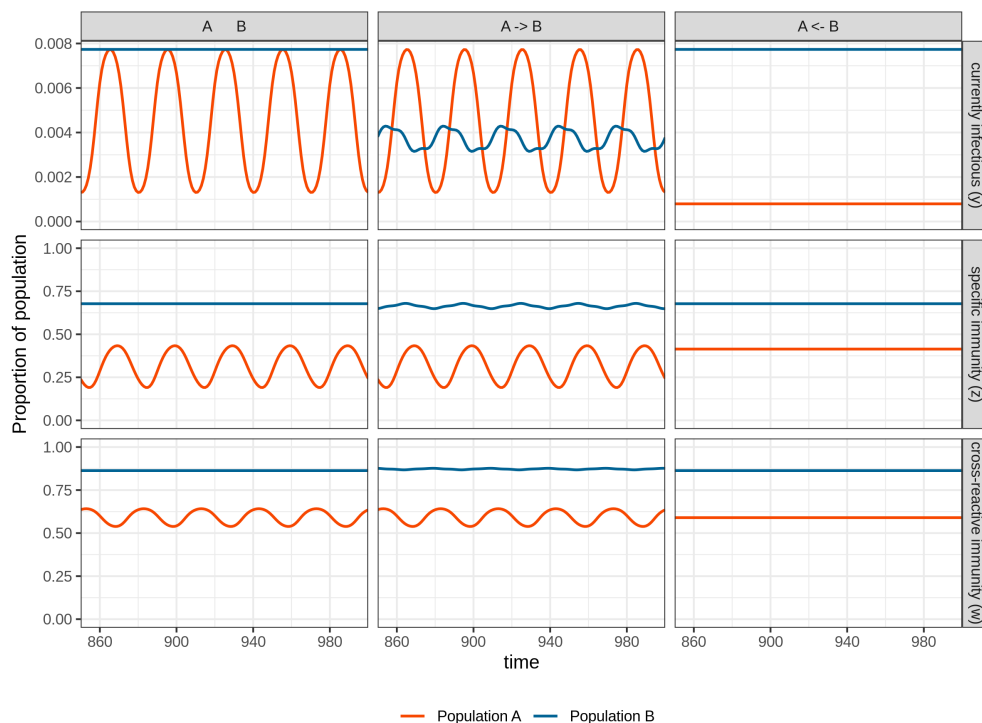
11

Figure 2: Destination populations tend to inherit origin population dynamics when linking populations with different model parametrizations. As in Fig 1, rows correspond to population classes, but here, columns indicate network structure. While in isolation (left column), population A has cyclical dynamics and population B has steady-state dynamics, when the two populations are linked by migration, the destination population inherits the dynamics of the origin population (center and right columns). This is true regardless of the direction of the movement (depending on the level of migration; see supporting information Fig S2). Populations A and B have parameters $\sigma = 8$, $\mu = 0.1$, $\delta = 0.05$, and $\gamma = 0.66$ in common and β chosen to reflect $\tilde{R}_0 = 2$ and 5, respectively. We use a two-loci, two-allele strain structure, but show only one strain for clarity.

3.3 Degree distribution affects pathogen prevalence and immunity

These simple patterns in the effects of origin population dynamics on those in the destination population have clear implications when pieced together into larger network structures. For instance, the propagation of immune individuals through the metapopulation suggests that populations further "up the chain" will tend to have higher on-average disease incidence and also greater variability. The inheritance of dynamical regimes combined with a hierarchy of dynamics in that inheritance suggests that chaos and cycles should be more common, especially in populations further "down the chain." That is, except in cases where the ultimate origin populations are all disposed toward
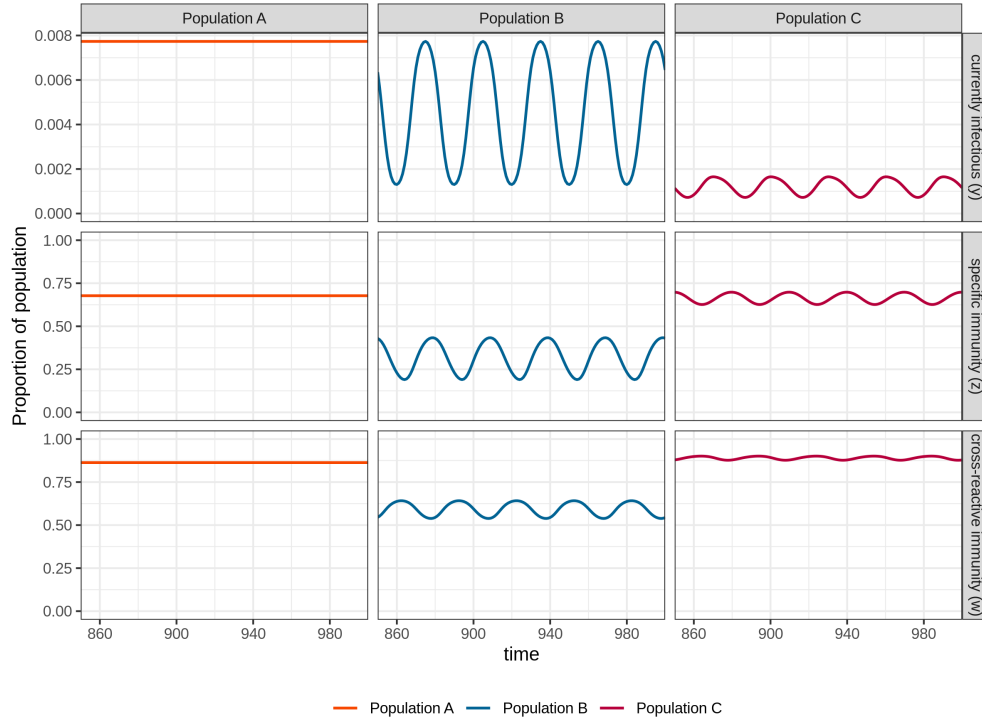
12

Figure 3: When multiple origin populations differ in their dynamics, the destination population inherits cycles over steady states. As in Fig 1, rows indicate population classes, and columns the component populations. Here, we have populations A and B feeding into population C at the same rate of $\delta = 0.05$. Populations A and C are parametrized to produce steady state dynamics in the absence of migration, with $\sigma = 8$, $\mu = 0.1$, $\gamma = 0.66$, and β corresponding to a $\tilde{R}_0 = 2$. Population B shows cyclical dynamics with β corresponding to a $\tilde{R}_0 = 5$ and all other parameters the same. Note that, even though the parameters of population C would lead to a steady state in the absence of migration, we see cyclical dynamics being inherited from population B. We use a two-loci, two-allele strain structure, but show only one strain for clarity.

²¹⁷ steady states, in which case the stabilizing effect could overrule downstream local parametrizations,

²¹⁸ leading to an overall stable system.

²¹⁹ In Fig 4, we report the effect of various network structures on three summary statistics of pathogen

²²⁰ prevalence (and levels of immunity) using five common network ensembles. Depending on the

²²¹ system being explored, empirical network structures might have elements in common with one or

²²² more of these ensembles, for instance, many social networks are considered to be "small-world" in

²²³ structure like Watts-Strogatz random graphs, while ecological networks are often commented on

²²⁴ for their formation of "modules" or clusters of more densely interacting species as in stochastic

225 block random graphs. Networks were parametrized to have approximately equal connectance and

226 size in order to reduce uninformative variation (see Section 2.3.3). This is because metapopulation

227 size and connectance have known effects on pathogen persistence, independent of further network

228 structure (23; 24; 25).

229 We found that the network configurations with higher variation in indegree (*i.e.* the number of

230 other populations each population receives migration from) distributions (supporting information

231 Fig S4), such as those found in the tree and Barabasi-Albert networks, tend to have higher levels

232 of infection over time, despite similar levels of immunity as the other three network types (Fig 4).

233 We saw similar patterns to those in infectious individuals when looking at time between epidemic

234 peaks across network types. While fewer of the populations ended up with cyclical dynamics in the

235 Barabasi-Abert graphs, the mean period of the cycles tended to be slightly higher and have higher

236 variance, but this was not robust to alternative parametrizations (supporting information Fig S5).
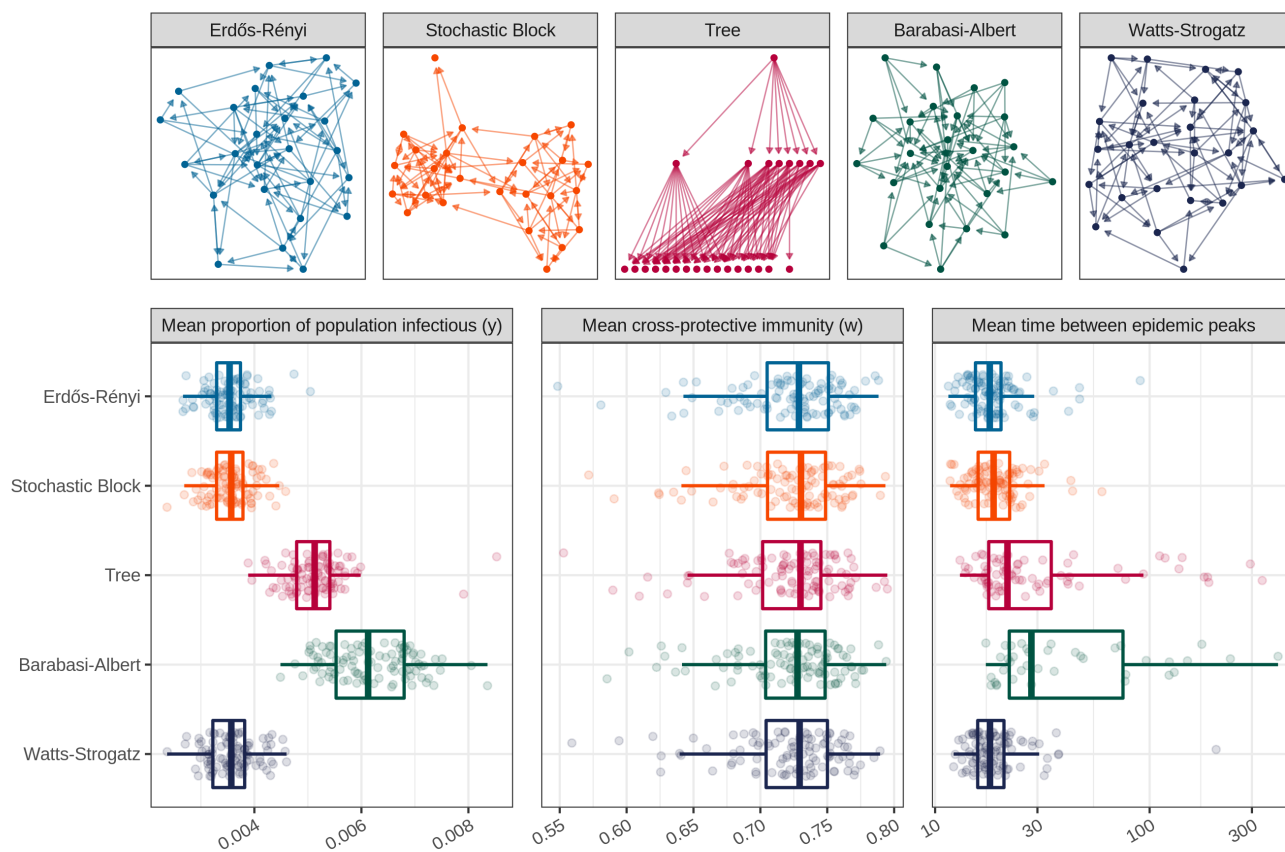
14

Figure 4: The effect of network structure on pathogen prevalence and levels of immunity through time. In the top row, we depict a representative network from each of the five ensembles. The second row shows the distributions of each of three response variables for prevalence of the pathogen and specific immunity over the course of the simulation, with the units for the horizontal axes given by the panel headings. We depict one point for each randomized network structure and box-plots indicating the median and inter-quartile range of each network-type's distribution. Network generating algorithms were tuned to produce networks of the same size and approximate connectance and model parameters were either the same for all populations and across simulations ($\sigma = 8$, $\mu = 0.1$, $\delta = 0.01$, and $\gamma = 0.66$) or randomized for each population in each simulation (initial densities of infectious and immune individuals [0, 1] and β value corresponding to a $\tilde{R}_0$ within [1, 6] for each population).

4   Discussion

Both metapopulation (26) and strain (16) structure have long been known to be important to disease dynamics and are increasingly being recognized as ubiquitous. Yet the combination of these two areas of theory has been underexplored. We show here that this lacuna can have real

15

²⁴¹ consequences for our understanding of disease dynamics in empirical systems.

²⁴² In probing the relationship between origin and destination dynamics in simple metapopulations,
²⁴³ we have demonstrated several patterns that expand our understanding of disease dynamics in
²⁴⁴ these systems. By directly incorporating a movement network into our model framework, we have
²⁴⁵ constructed a very general approach that lends itself to arbitrarily large and complex systems.
²⁴⁶ This is noteworthy, as more and more natural systems are being thought of in terms of networks
²⁴⁷ of interacting components (*e.g.* separate species in ecological communities (27) or host individuals
²⁴⁸ exchanging parasites (28)). By adjusting the scale of our metapopulation, we can ask and answer
²⁴⁹ different questions about the forces influencing disease dynamics.

²⁵⁰ We found that the dynamics of prevalence and immunity among migrationally connected popu-
²⁵¹ lations are not independent, and that even very small rates of population movement can have
²⁵² profound effects on a population's disease dynamics: from reducing pathogen prevalence to chang-
²⁵³ ing the dynamical regime of destination populations entirely. Our findings regarding the reduction
²⁵⁴ in cycle amplitude (Section 3.1) echo results in dispersal networks in ecology, where population
²⁵⁵ dynamics were dampened following the introduction of migration (29).

²⁵⁶ Contrary to prior focus in the literature on the role of migrating infectious individuals (30; 31;
²⁵⁷ 26), we found that the migration of immune individuals can be equally (or even more) important.
²⁵⁸ This is noteworthy, as the few previous studies relating multi-strain diseases and metapopulation
²⁵⁹ structure only allow pathogen transmission between populations, not the movement of individuals
²⁶⁰ explicitly (3; 32)—an approach that is more mathematically tractable, but omits the potentially
²⁶¹ influential transmission of immune individuals.

²⁶² Finally, we show that larger network structure also has a part to play in disease dynamics, resulting
²⁶³ in significant differences in pathogen prevalence across network types. Our results are in agreement
²⁶⁴ with previous results suggesting increased epidemic size in scale-free network structures (such as
²⁶⁵ those found in Barabasi-Albert random graphs) when the spreading rate is sufficiently slow (33;
²⁶⁶ 34) due to the high-degree nodes serving as "super-spreaders" (35; 25). Along these lines, there
²⁶⁷ has been some previous research indicating that node degree (the number of other populations a

16

given population is connected to) is directly related to pathogen prevalence in that focal population ((36), but see (37)), however a complete investigation into network structure at the node-level is beyond the scope of this work. A comprehensive investigation of the role of more complex network structures in disease dynamics, however, remains a topic for further investigation.

In this work, we have utilized a relatively simple model for disease dynamics in an effort to maximize interpretability. Such simplification inevitably comes with a cost, and several of our assumptions can be critiqued as unrealistic. Perhaps foremost is the assumption of continuous movement. While continuous movement might be appropriate for very large populations with frequent, relatively small migrations between them, when any of these three components is not present, we would expect deviation from these predictions. Future work could explore the importance of discrete movement regimes on these patterns. Likewise, in this work we omit strain mutation and recombination (17) (yet the latter is included in the original framework of (16)). The generation of novel strains is likely important to the global persistence of diseases in humans (38) and animals (39). Finally, in representing movement by adding a proportion of the origin population to the destination, we introduce an assumption that the two populations in question are of approximately the same size. In a metapopulation where populations vary widely in size, the proportion leaving one population would not correspond to the proportion entering another.

This work should not be seen as an attempt at comprehensive categorization of the role of meta-population structure on the dynamics of multi-strain diseases, but rather as an initial step in exploring the complex interplay between the population structure of hosts and strain structure of pathogens. Our results suggest there may be simple rules underlying this relationship, at least for a wide range of parameter values, but it remains to be seen where networks based on empirical data fall in these parameter regimes, as well as how such systems might deviate from theoretical expectations.

17

5   Acknowledgments

We would like to thank José Lourenço for helpful discussions regarding the mathematical framework of this work. This work was supported by the USDA National Institute of Food and Agriculture, Animal Health project #MINV-62-057.
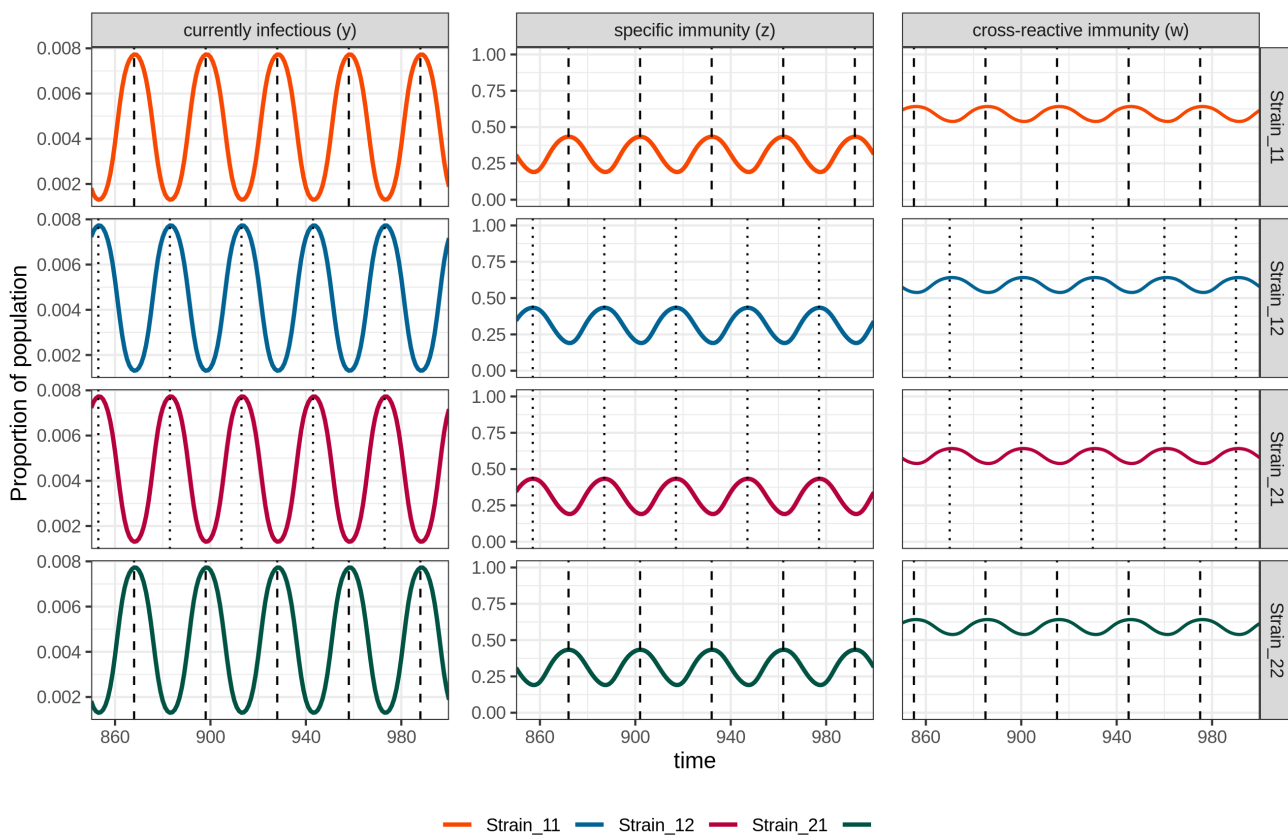
S1   Supporting Information

Figure S1: Considering all the dynamics of all four strains from population A in Fig 1. Note that lines are colored according to strain rather than population. Strains can be divided into two discordant sets of non-overlapping alleles: {1, 1} and {2, 2}, and {1, 2} and {2, 1}. Each strain of a discordant set behaves identically due to identical parametrization and no interaction between strains that do not share at least one allele, but discordant sets interact with one another due to partial cross-reactive immunity. Thus, when one set is abundant, the other is rare and *vice versa*. We highlight the maximum value of each discordant set's cycle with a vertical line in order to facilitate comparisons between strains and sets.
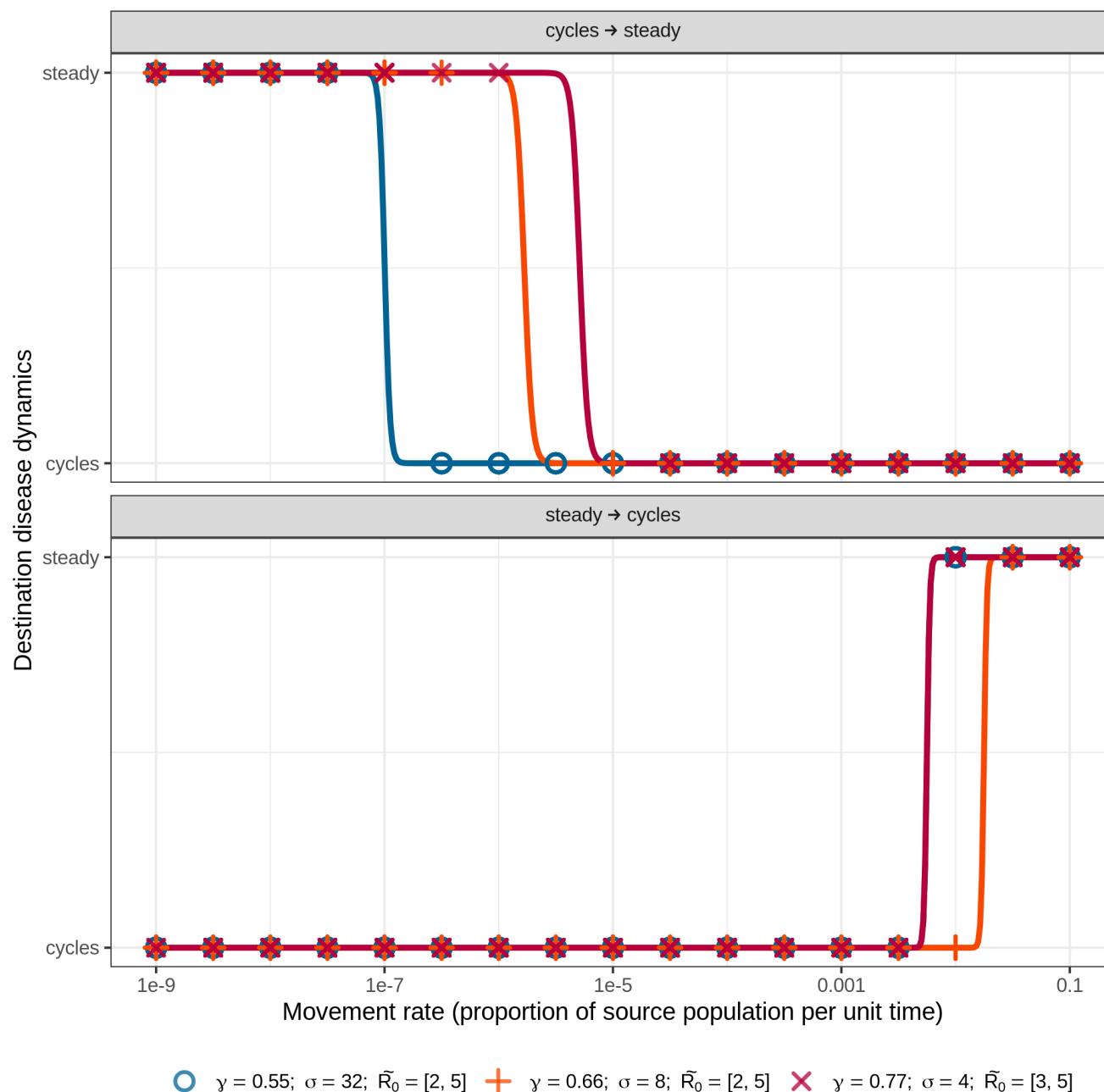
Figure S2: The effect of variable migration rate on transference of dynamical regime from origin to destination in a simple metapopulation of two populations linked by unidirectional movement. In the top panel are cases where the origin population has cyclical dynamics and the destination has steady state dynamics when in isolation, while in the bottom panel the opposite is true. As the movement rate (δ· horizontal axis) increases, there is a phase-transition at which point the destination population's dynamics (indicated by the vertical axis) switch to match those of the origin. We fit a binomial spline to highlight this transition point. We see that even with very small rates of migration, a stable population can be converted to a cyclical one (top panel). Yet, it is more difficult to convert a cyclical population to one with steady state dynamics (bottom panel). Three parametrizations are recorded here (color; see legend), with additional parameter μ = 0.15 being the same for both populations. Finally, note that the two values of $\tilde{R}_0$ listed in the legend correspond to the two populations, with the larger value corresponding to the steady state population and the smaller value the cyclical population (when in isolation) .
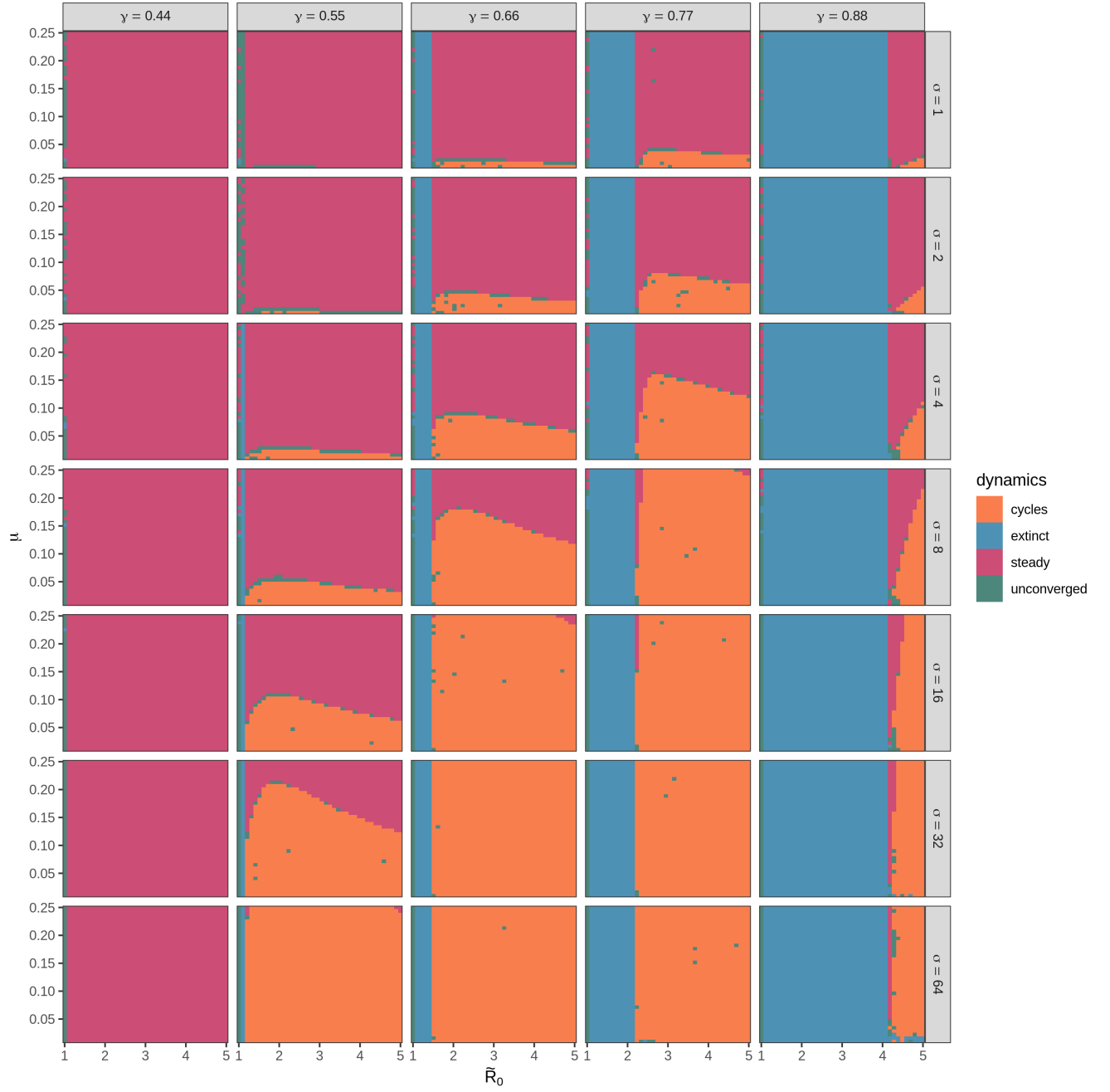
20

Figure S3: Effect of parametrization on dynamic regime for a population in isolation. Here, columns indicate values of γ and rows indicate values of σ. Depending on the combination of β, σ, μ, and γ, a population can exhibit a range of dynamics including steady states for all strains (pink), cyclical or chaotic dynamics for all strains (orange), or partial extinction of some strains (blue). Green cells indicate a numerical failure in integration. All simulations here utilize a two-loci, two-allele strain structure. See (16) for a similar figure for alternative parameterizations.
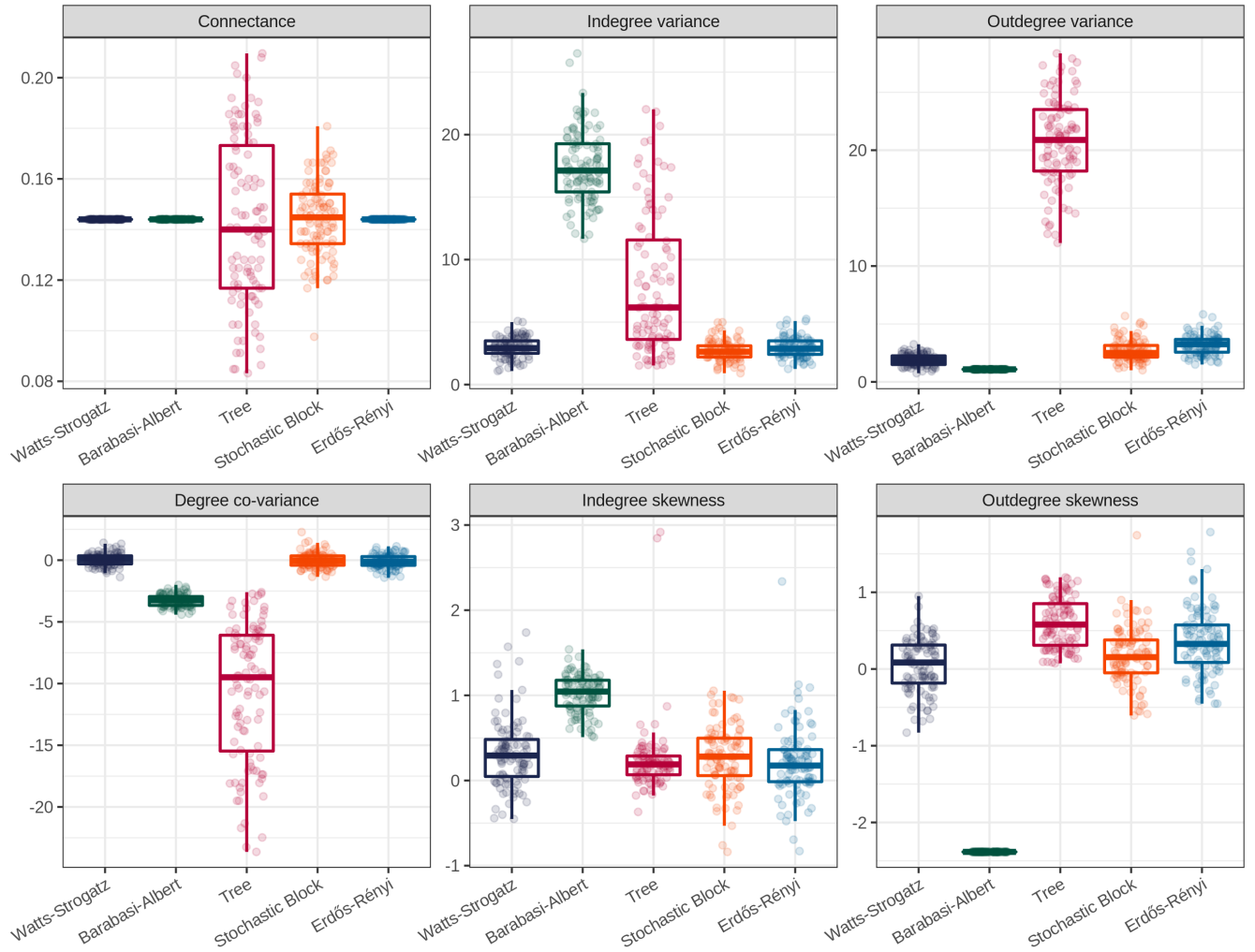
Figure S4: Summary statistics for the degree distributions of each randomized network used for Fig 4 in the main text. Networks were constructed to have the same size and approximate connectance, but with the network structure (which populations are connected to which other popuations) otherwise generated according to one of five algorithms: Erdős-Rényi, Barabasi-Albert, and Watts-Strogatz, stochastic block, and tree (see Section 2.3.3 of the main text). Some algorithms allowed perfect matching of connectance (Erdős-Rényi, Barabasi-Albert, and Watts-Strogatz), while others necessitated some minor variation (stochastic block and tree).

Figure S5: Similar to the lower row of Fig 4,but with γ and σ equal to 0.55 and 32, respectively. All other parameters are equal to or set randomly as in Fig 4. All other parameters are equal to or set randomly as in Fig 4. While the observed differences in total infected are robust, note that here the mean time between epidemic peaks is approximately equal across randomizations.

References

1. Couch RB, Kasel JA. Immunity to influenza in man. Annual review of microbiology. 1983;37(1):529–49.

2. Castillo-Chavez C, Hethcote HW, Andreasen V, Levin SA, Liu WM. Epidemiological models with age structure, proportionate mixing, and cross-immunity.. J Math Biol. 1989;27:233–58.

3. Lourenço J, Recker M. Natural, persistent oscillations in a spatial multi-strain disease system with application to dengue.. PLoS Comput Biol. 2013;9:e1003308.

4. Wilson EO, MacArthur RH. The theory of island biogeography. Princeton University Press; 1967.

5. Taylor AD. Large-scale spatial structure and population dynamics in arthropod predator-prey systems. Annales Zoologici Fennici. 1988;:63–74.

6. Hanski I. A practical model of metapopulation dynamics. The Journal of Animal Ecology. January 1994;63(1):151.

7. Hess G. Disease in metapopulation models: implications for conservation. Ecology. July 1996;77(5):1617–32.

8. Cross PC, Lloyd-Smith JO, Johnson PLF, Getz WM. Duelling timescales of host movement and disease recovery determine invasion of disease in structured populations. Ecology Letters. June 2005;8(6):587–95.

9. Lloyd AL, Jansen VAA. Spatiotemporal dynamics of epidemics: synchrony in metapopulation models. Mathematical Biosciences. March 2004;188(1-2):1–16.

10. Ruxton GD. Low levels of immigration between chaotic populations can reduce system extinctions by inducing asynchronous regular cycles. Proceedings of the Royal Society of London Series B: Biological Sciences. May 1994;256(1346):189–93.

11. Earn DJD, Rohani P, Grenfell BT. Persistence chaos and synchrony in ecology and epi-

demiology. Proceedings of the Royal Society of London Series B: Biological Sciences. January 1998;265(1390):7–10.

12. Hanski I. Metapopulation dynamics. In: Metapopulation Biology. Elsevier; 1997. p. 69–91.

13. Brown JH, Kodric-Brown A. Turnover Rates in Insular Biogeography: Effect of Immigration on Extinction. Ecology. March 1977;58(2):445–9.

14. Rosenzweig ML. Paradox of Enrichment: Destabilization of Exploitation Ecosystems in Ecological Time. Science. January 1971;171(3969):385–7.

15. Hilker FM, Schmitz K. Disease-induced stabilization of predator–prey oscillations. Journal of Theoretical Biology. December 2008;255(3):299–306.

16. Gupta S, Ferguson N, Anderson R. Chaos persistence, and evolution of strain structure in antigenically diverse infectious agents. Science. May 1998;280(5365):912–5.

17. Lourenço J, Wikramaratna PS, Gupta S. MANTIS: an R package that simulates multilocus models of pathogen evolution. BMC Bioinformatics. May 2015;16(1).

18. Xiao Y, Zhou Y, Tang S. Modelling disease spread in dispersal networks at two levels. Mathematical Medicine and Biology. September 2011;28(3):227–44.

19. Bezanson J, Edelman A, Karpinski S, Shah VB. Julia: a fresh approach to numerical computing. SIAM Review. January 2017;59(1):65–98.

20. Wickham H. ggplot2: Elegant Graphics for Data Analysis. Springer-Verlag New York; 2016.

21. R Core Team. R: a language and environment for statistical computing. Vienna, Austria: R Foundation for Statistical Computing; 2019.

22. Pedersen TL. tidygraph: a tidy API for graph manipulation. 2019.

23. Ganesh A, Massoulié L, Towsley D. The effect of network topology on the spread of epidemics. In: Proceedings IEEE 24th Annual Joint Conference of the IEEE Computer and Communications Societies. IEEE; 2005. p. 1455–66.

24. Salathé M, Jones JH. Dynamics and control of diseases in networks with community structure.. PLoS Comput Biol. 2010;6:e1000736.

25. Keeling MJ, Eames KTD. Networks and epidemic models. Journal of The Royal Society Interface. June 2005;2(4):295–307.

26. Grenfell B, Harwood J. (Meta)population dynamics of infectious diseases. Trends in Ecology & Evolution. October 1997;12(10):395–9.

27. Proulx SR, Promislow DE, Phillips PC. Network thinking in ecology and evolution.. Trends Ecol Evol. 2005;20:345–53.

28. Craft ME, Caillaud D. Network models: an underutilized tool in wildlife epidemiology?. Interdiscip Perspect Infect Dis. 2011;2011:676949.

29. Holland MD, Hastings A. Strong effect of dispersal network structure on ecological dynamics.. Nature. 2008;456:792–4.

30. Jesse M, Ezanno P, Davis S, Heesterbeek JAP. A fully coupled mechanistic model for infectious disease dynamics in a metapopulation: Movement and epidemic duration. Journal of Theoretical Biology. September 2008;254(2):331–8.

31. North AR, Godfray HCJ. The dynamics of disease in a metapopulation: The role of dispersal range. Journal of Theoretical Biology. April 2017;418:57–65.

32. Wikramaratna PS, Pybus OG, Gupta S. Contact between bird species of different lifespans can promote the emergence of highly pathogenic avian influenza strains.. Proc Natl Acad Sci U S A. 2014;111:10767–72.

33. Pastor-Satorras R, Vespignani A. Epidemics and immunization in scale-free networks. In: Handbook of Graphs and Networks [Internet]. Wiley-VCH Verlag GmbH & Co. KGaA; 2004. p. 111–30. Available at: https://doi.org/10.1002%2F3527602755.ch5

34. Lloyd-Smith JO, Schreiber SJ, Kopp PE, Getz WM. Superspreading and the effect of individual variation on disease emergence.. Nature. 2005;438:355–9.

25

35. Shirley MDF, Rushton SP. The impacts of network topology on disease spread. Ecological Complexity. September 2005;2(3):287–99.

36. Godfrey SS, Bull CM, James R, Murray K. Network structure and parasite transmission in a group living lizard the gidgee skink, Egernia stokesii. Behavioral Ecology and Sociobiology. April 2009;63(7):1045–56.

37. VanderWaal KL, Atwill ER, Hooper S, Buckle K, McCowan B. Network structure and prevalence of Cryptosporidium in Belding's ground squirrels. Behavioral Ecology and Sociobiology. July 2013;67(12):1951–9.

38. Antia R, Regoes RR, Koella JC, Bergstrom CT. The role of evolution in the emergence of infectious diseases. Nature. December 2003;426(6967):658–61.

39. Tompkins DM, Carver S, Jones ME, Krkošek M, Skerratt LF. Emerging infectious diseases of wildlife: a critical perspective.. Trends Parasitol. 2015;31:149–59.